Dynamical mean-field solution of coupled quantum wells: A bifurcation analysis

Jorge Galán and Emilio Freire
Departamento de Matemática Aplicada II, Escuela Superior de Ingenieros, Camino de los Descubrimientos s/n, 41092 Sevilla, Spain
(Received 18 May 2000; published 26 September 2001)

The time evolution of a discrete model of three quantum wells with a localized mean-field electrostatic interaction has been analyzed making use of numerical simulation and bifurcation techniques. The discrete Schrödinger equation can be written as a classical Hamiltonian system with two constants of motion. The frequency spectrum and the Lyapunov exponents show that the system is chaotic as its continuum counterpart. The organizing centers of the dynamical behavior are bifurcations of rotating periodic solutions whose simple structure allows a thorough analytical investigation as the conserved quantities are varied. The global structure of the periodic behavior is organized via subharmonic bifurcations at which tori of nonsymmetric periodic solutions are born. We have found another kind of bifurcation when two pairs of characteristic multipliers split from the unit circle. The chaotic behavior is related to the nonintegrability of the system.

DOI: 10.1103/PhysRevE.64.046220 PACS number(s): 05.45.−a, 71.10.Fd, 03.65.−w

I. INTRODUCTION

The mean-field approximation is the starting point for most of the theoretical calculations in which more than one charged quantum particle is present: quantum statistical physics, electronic-structure calculations, strongly correlated systems, quantum transport, atomic and nuclear systems, etc. The many-body electrostatic interaction is replaced by an average value of the field created by all the particles acting on one of them [1]. For a one-dimensional and unforced system, the Hamilton operator is time independent and the Schrödinger equation in the mean field approximation can be written as

$$i\hbar\dot{\Psi}(x,t)=\hat{H}_{\mathrm{mf}}(|\Psi(x,t)|,x)\Psi(x,t), \tag{1}$$

where $\Psi(x,t)$ is the wave function and H_{mf} is the mean field approximation of the Hamilton operator.

The usual way to analyze the problem is by separation of variables. The wave function is factorized as a product of a temporal and a spatial term, $\Psi(x,t)=e^{-i\hbar\omega t}\phi(|\Psi|,x)=e^{-i\hbar\omega t}\phi(|\phi|,x)$. The spatial part ϕ is the solution of a nonlinear integro-differential eigenvalue equation,

$$\hat{H}_{\mathrm{mf}}(|\phi(x)|,x)\phi(x)=\hbar\omega\phi(x), \tag{2}$$

which can be solved with an iterative self-consistent method. The resulting wave function is the Hartree solution of the system and it is known to have the lowest energy among all possible factorized trial functions [1]. The wave function representing the whole system is finally constructed taking into account the kind of particles involved (fermions or bosons) (Hartree-Fock solution).

Within this approach, the dynamical behavior of the system is frozen, because all the expectation values are time independent and, in particular, the *stability* of the mean field solution is not directly available. However, there is another possible approach to the time-dependent mean field problem, namely, to consider solutions in which the time and spatial dependence are not factorized in the wave function and some of the expectation values are allowed to vary in time. From the variational point of view, the class of wave functions that are considered is more general than the Hartree one.

This second dynamical mean field approach was used by the authors of Ref. [2] to investigate a specific example, namely the time evolution of a wave packet in a three-quantum-well device including a mean field electrostatic interaction in the middle well, as shown schematically in the upper part of Figure 1. The physical image is easy to understand: an initially localized wave packet representing a cloud of electrons in a noninteracting well is diffused across the central barriers and reflected elastically back and forth by the outermost barriers. The central well is narrower and in it the electrostatic interaction is not negligible. Electrons in this region have higher energy and are kicked out of it. This problem is interesting from the fundamental point of view and because it is a toy model for actual semiconductor devices such as quantum wells or quantum dots.

In [2] it was shown, by *numerical simulations* and appropriate values of the parameters, that the dynamical behavior of the total charge in the central well is chaotic after a transient time. They called this effect ''chaotic quantum phenomena without classical counterpart,'' and characterized the chaotic dynamical behavior by statistical indicators (correlation functions, power spectra, information dimension, and

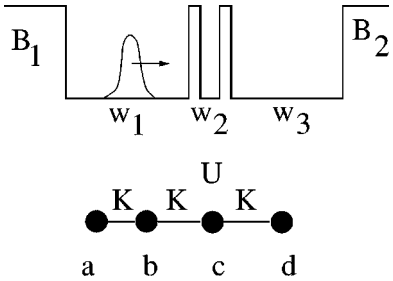

FIG. 1. Schematic representation of the potential profile [$V(x)$ in Eq. (4)] (top). B_1 and B_2 are infinite potential barriers that confine the particles into the well region. The wave packet represents the initial condition and w_2 is a narrow well separated by finite barriers where the electrostatic interaction is non-negligible. The bottom figure shows the discrete four site system of Eq. (5).

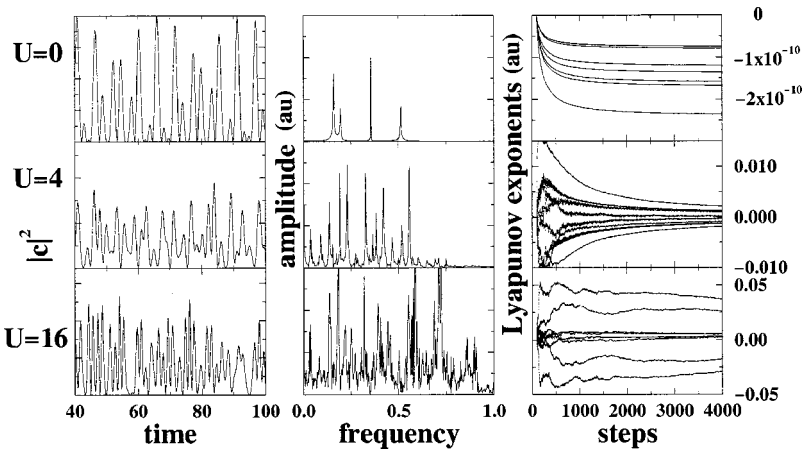

FIG. 2. Numerical results by simulation of Eqs. (4), $K=1$, and the same initial conditions. The upper row is the linear case ($U=0$), the middle row is for $U=4$, and the lower one is for $U=16$. The left column is the temporal evolution of the charge on the third site; $|c(t)|^2$. The central column is the Fourier spectrum of the signal and the right one shows the eight Lyapunov exponents. For $U=0$, the system is quasiperiodic, whereas for $U=4$ and $U=16$ it is chaotic.

entropy). In a subsequent publication [3], the same authors proposed a discrete three-site model representing the same physical system that also exhibited chaotic behavior only when the nonlinearity introduced by the mean field term is *not homogeneous* in space.

In this work, we derive an appropriate discrete model that reproduces the chaotic behavior and allows a thorough analytical investigation. We have focused on the *geometrical* and *qualitative* description of the dynamics performing a bifurcation analysis, in contrast to the above-mentioned numerical and statistical characterizations. We show that the dynamical behavior is rich and give an explanation of the importance of the position of the nonlinearity in the three-site case.

The structure of the paper is the following. In Sec. II, we introduce the continuum model and its reduction to a finite-dimensional tight-binding mean field model. In Sec. III, we show by numerical simulation of the equations that this discrete model retains the chaotic features of its continuum counterpart. The core of our work comes in Sec. IV. There, we show that by taking advantage of the Hamiltonian structure of the discrete equations and the role of the symmetry and the associated conserved quantities, we can identify bifurcations of families of periodic orbits as organizing centers for the dynamical behavior of the system. Finally, in Sec. V we summarize and discuss possible physical implications of our results.

II. MODEL AND EQUATIONS

The nonlinear one-dimensional Schrödinger equation [2] in the mean field approximation describing the evolution of the electron wave function in a three-quantum-well system is

$$i\hbar\frac{\partial\Psi(x,t)}{\partial t}=-\frac{\hbar^2}{2m}\frac{\partial^2\Psi(x,t)}{\partial x^2}+[V(x)+\alpha Q(t)\chi(x)]\Psi(x,t), \qquad (3)$$

where $V(x)$ is the potential profile shown in the upper part of Fig. 1, $Q(t)=\int_{w_2}|\Psi(x,t)|^2dx$ is the electronic charge in the central well (w_2), χ is a characteristic function that is one within well w_2 and zero elsewhere, and α measures the electrostatic coupling.

Following the standard tight-binding approach [1], we simplify the partial differential equation and reduce it to a system of complex ordinary differential equations by retaining only a kinetic energy term and a local electrostatic repulsion between electrons and parametrize them by $-K$ and U, respectively. As these contributions should have opposite signs, we take K and U real and positive. This reduction process is similar to the derivation of the Hubbard or Anderson model in condensed-matter physics [4]. The spin of the electron has been ignored but could be included by doubling the dimension of the problem. The natural number of sites to use would be three and would include the nonlinear mean field term in the second site, but as we will show in Sec. IV A, the resulting system is *integrable* and unable to reproduce the chaotic behavior present in the continuum model. In this work, we consider a four-site system (lower part of Fig. 1), with two sites at one side of the interacting one and just one site on the other side. The nonlinear interaction is present only in the third site (marked by c in Fig. 1). We get the following discrete time-dependent Schrödinger equation:

$$\begin{aligned}\dot{a}&=iKb,\\ \dot{b}&=iKa+iKc,\\ \dot{c}&=iKb+iKd-iU\bar{c}c^2,\\ \dot{d}&=iKc,\end{aligned} \qquad (4)$$

where a, b, c, and d are complex functions of time representing the components of the wave function on each site. Note that the equations are linear apart from the U term and the kinetic part is just the nearest-neighbor hopping matrix in an open one-dimensional four-site chain.

III. CHAOTIC BEHAVIOR: FOURIER SPECTRUM AND LYAPUNOV EXPONENTS

A first approach to identify chaotic behavior in Eqs. (4) is to integrate them numerically for given values of the parameters U and K and an initial condition, in an analogous way to what was done in Ref. [2]. In Fig. 2, we plot different

magnitudes for three values of the on-site interaction U. The upper row is for the noninteracting case $U=0$, the middle row for $U=4$, and the bottom one for $U=16$. The first column is the temporal evolution of the charge in well c in a window of 60 units of time after a transient, the second one is the power spectra of the previous column computed in a much broader time interval, and the last one is the eighth Lyapunov exponent [5]. In all cases, we fixed $K=1$ and started the simulation from the same initial condition: $a(0)=1$, $b(0)=c(0)=d(0)=0$.

For the noninteracting case, the system is linear and it is straightforward to show that $c(t)$ is a linear combination of $\cos(\phi t)$ and $\cos(\frac{t}{\phi})$, where $\phi=(1+\sqrt{5})/2$ is the golden mean number. Therefore, in $|c(t)|^2$ we find only contributions of four incommensurate frequencies: 2ϕ, $2/\phi$, $\phi+1/\phi$ and $\phi-1/\phi$. Generically, the trajectories are *quasiperiodic*. The position of the four peaks in the power spectra in the second column coincides with the predictions and, as expected, the Lyapunov exponents for a linear system are zero (note that the vertical scale for this case is 10^{-10}).

For intermediate values of the interaction ($U=4$), the temporal signal does not show a quasiperiodic behavior and the Fourier spectra exhibit numerous peaks. The system behaves *qualitatively* different from the linear case. The Lyapunov exponents (one for each variable) appear always in pairs $\lambda_i, -\lambda_i$ and at least two of them are zero. Note that this fact is an outcome of our calculation because the algorithm used [5] does not take advantage of the fact that the system is conservative.

In the strong interacting case ($U=16$), the signal does not seem to follow any pattern and the power spectra are relatively broad and peaked. Two of the Lyapunov exponents are positive and we can affirm that the dynamical behavior is *chaotic*.

IV. BIFURCATION ANALYSIS

The previous analysis indicates that our discrete model is able to describe the chaotic behavior present in the continuum case. In this section, we will show that we can extract additional information about our system by standard bifurcation techniques.

We can render system (4) free of parameters by taking $K>0$ as a time unit and rescaling each variable by $\sqrt{U/K}$. Note that $U=0$ corresponds to the linear case and $K=0$ is a frozen system in which the particles are not allowed to jump from one site to its neighbor. This scaling analysis shows, as expected, that the interaction strength is equivalent to total charge. The resulting system is

$$\begin{aligned}\dot{a}&=ib,\\ \dot{b}&=ia+ic,\\ \dot{c}&=ib+id-i\bar{c}c^2,\\ \dot{d}&=ic.\end{aligned}\tag{5}$$

The parameters in the problem are the energy and the total charge that are not present in the equations but are fixed by the initial condition. Equations (5) can be written as a classical Hamiltonian system as

$$\dot{z}=i\frac{\partial H(z,\bar{z})}{\partial \bar{z}},\tag{6}$$

$$H(z,\bar{z})=(a\bar{b}+\bar{a}b+b\bar{c}+\bar{b}c+c\bar{d}+\bar{c}d)-\frac{(c\bar{c})^2}{2},\tag{7}$$

with $z=(a,b,c,d)$. The Hamiltonian is *autonomous*, *reversible* [$H(z,\bar{z})=H(\bar{z},z)$], and *invariant under diagonal rotations* in $\mathcal{C}^4$ ($z\rightarrow ze^{i\theta}$).

A direct application of Noether's theorem shows that there are at least two independent conserved quantities in the problem associated to the symmetries: the energy which is equal to the Hamiltonian and the total charge (norm of the state vector),

$$n_t=z\bar{z}=a\bar{a}+b\bar{b}+c\bar{c}+d\bar{d}.\tag{8}$$

This second constant of motion is related to the gauge invariance of Schrödinger's equation or, equivalently, to the fact that the system is closed. The time independence of $z\bar{z}$ can be proven from the invariance condition as follows:

$$H(e^{i\theta}z,e^{-i\theta}\bar{z})=H(z,\bar{z}),\quad \forall\,\theta\in\mathcal{R}.\tag{9}$$

Derivating with respect to θ and using the chain rule,

$$\frac{\partial H}{z}iz+\frac{\partial H}{\bar{z}}(-i)\bar{z}=0.\tag{10}$$

Substituting Eq. (6) and its complex conjugate,

$$\dot{\bar{z}}z+\dot{z}\bar{z}=0\Rightarrow\frac{d}{dt}(z\bar{z})=0.\tag{11}$$

A. Integrability of the three-site model

If we take three sites in the discrete model and consider the nonlinear term in the middle one, then the first and third equations have the same right-hand side, namely $\dot{a}=ib$ and $\dot{c}=ib$. Therefore, a and c only differ in an initial value. However, the system still has the two independent constant of motion and the dynamical behavior is restricted to a $6-2-2=2$ dimensional space. In conclusion, for three sites and the nonlinear term in the central site, the discrete model exhibits only periodic or quasiperiodic solutions. One possibility to destroy the integrable character is to break the symmetry between the first and third well. This approach was followed in [3] by displacing the nonlinear term to one of the end sites and calling it a *nonhomogeneous* nonlinearity. Another straightforward solution is to increase the dimension of the system by adding more sites at one side of the nonlinear term. This is the approach chosen in the present work, as explained above. The reason for this selection is to preserve the original structure of the quantum-well problem, but our results can be readily translated to the nonhomogeneous three-site case.

From the results of Sec. III, we have *numerical evidence* that the four-site system is *nonintegrable*. The rest of our work will be devoted to the bifurcation analysis of system (5). We will see that the Hartree solutions mentioned in the Introduction play a central role in the understanding of the dynamical behavior of the system.

B. Equilibrium

The only equilibrium point of Eqs. (5) is the origin and corresponds to the case of an empty system. Separating in real and imaginary parts, the system is eight-dimensional and the spectrum of the linearization is

$$\sigma = i\left\{\phi, -\phi, \frac{1}{\phi}, -\frac{1}{\phi}, -\phi, \phi, -\frac{1}{\phi}, \frac{1}{\phi}\right\} \tag{12}$$

with $\phi=(1+\sqrt{5})/2$ and, because the Jacobian is symmetric, the eigenvalues are semisimple.

By the Lyapunov center theorem [6], we know that there exists four one-parameter families of periodic orbits. Moreover, when approaching the origin along the families, the periods tend to $2\pi/\lambda_i$ and the nontrivial characteristics multipliers tend to $\exp(2\pi\lambda_j/\lambda_i)$ for $j\neq i$ and $i=1,2,3,4$. It is well known that for Hamiltonian systems the periodic orbits are densely distributed among all possible classical trajectories and that they are the key to the overall behavior of any mechanical system. Periodic orbits form continuous families in phase space that can be investigated by varying either the energy of the system or some external parameter.

A classical theorem by Weinstein [7] ensures, under a certain hypothesis, the existence of at least N families of periodic orbits in an N degrees of freedom Hamiltonian system. In our case and due to the presence of resonances, we might expect more families of periodic orbits than those four born at the origin.

C. Perturbation theory: Hamiltonian normal form

A common approach for low values of the interaction in the original many-body system is to perform a perturbative study in U/K in the unscaled equations (4); the starting point is the noninteracting case and the interaction is adiabatically introduced. The mean field approximation corresponds to the first-order perturbative correction for low values of U/K [8,9]. Within this method, we can study the four families of a periodic orbit that are born in the origin. In the scaled system (5), the perturbative analysis is equivalent to studying the neighborhood of the origin in $\mathcal{R}^8$.

In the classical Hamiltonian formalism, there is a systematic and powerful tool to study the dynamics in the neighborhood of invariant objects such as equilibrium points, periodic orbits, or invariant tori, namely the Hamiltonian normal form. It provides a nonlinear approximation, usually in the form of asymptotic series, that includes only the higher-order terms that are essential for the bifurcation analysis.

This method has the advantage of not only providing the correction to the invariant object and its stability, but also, in principle, detecting other families of solutions that may exist close to the object [10]. They have been used to compute invariant manifolds [11], invariant tori [12], or to produce estimates on the diffusion time near linearly stable invariant objects [13–15].

To compute the Hamiltonian normal form around the origin, we perform nonlinear changes of variables such that the transformed equation will be in the simplest possible form, so that the essential features of the flow near the critical point become more evident. The desired simplification will be obtained, up to terms of a specified order; by performing inductively a sequence of near identity change of coordinates [16].

By a symplectic change of variables, we put the original Hamiltonian into the form $H=H_2+H_k+\tilde{H}$, where H_2 is the quadratic part, H_k is of degree $\leqslant k$, and $\tilde{H}$ is of order $>k$.

The Birkhoff-normal form [16] up to order 4 contains only the resonant monomials x^α,

$$\sum_{i=1}^{4} \lambda_i(\alpha_i-\alpha_{i+4})=0,$$

where α is a multi-index. Taking into account the symmetry and the reversibility, we get

$$\begin{aligned} H=&\phi(a\bar{a}-b\bar{b})+\frac{1}{\phi}(c\bar{c}-d\bar{d})-\frac{1}{(4+2\phi)^2}[\phi^4(a\bar{a})^2 \\ &+\phi^4(b\bar{b})^2+(c\bar{c})^2+(d\bar{d})^2+4\phi^2(a\bar{a}b\bar{b}+a\bar{a}c\bar{c} \\ &+a\bar{a}d\bar{d}+b\bar{b}c\bar{c}+b\bar{b}d\bar{d})+4c\bar{c}d\bar{d} \\ &+4\phi^2(ab\overline{cd}+\overline{ab}cd)], \end{aligned} \tag{13}$$

where the state vector is in the diagonal basis of the linearization of H around the origin. The symmetry of the problem imposes the same sign for all the quartic terms. Following the analysis of Sanders and Verhulst [10], we have found that the only periodic solutions that exist close to the equilibrium are the four families of periodic orbits predicted by the Lyapunov center theorem.

A general approach to find periodic orbits in Hamiltonian systems by continuation of periodic orbits of the linearized system around an elliptic point (nonlinear modes) and to investigate its stability has recently been presented in [17].

We can study the periodic orbits in a Hamiltonian system by continuation of the periodic orbits of the linearized system around an elliptic point (nonlinear modes) as follows: If H is in Birkhoff-normal form, the S^1 orbits of critical points of $H_\tau=2\pi[-\tau H_2+H_k]$ near the equilibrium point are periodic trajectories of the system with period $2\pi/[\lambda_i(1+\tau)]$ [17]. Moreover, the characteristic exponents can be computed by diagonalizing the linear part of the H_τ flow $JD^2H_\tau(u(0))$; where $J=\left(\begin{smallmatrix}\mathcal{O} & -\mathcal{I}\\ \mathcal{I} & \mathcal{O}\end{smallmatrix}\right)$, $\mathcal{I}$ and $\mathcal{O}$ are the identity and zero matrices of order 4, respectively, and $u(t)$ is the periodic orbit close to the origin. The characteristic multipliers are just the exponential of the exponents times the period of the orbit.

In Fig. 3, we present a comparison for the characteristic multipliers as a function of n_t computed from the normal

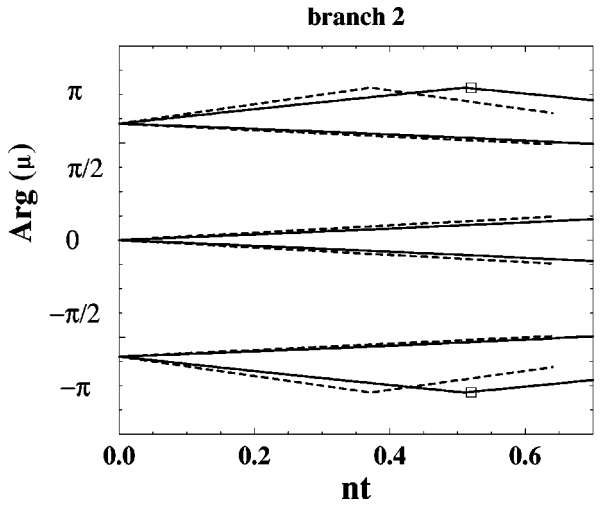

FIG. 3. Comparison of the significant characteristic multipliers (μ_i) as a function of the total charge (n_t) computed from the normal form (dashed line) and the exact ones (solid line), for the second branch of periodic solutions that emanates from the origin. In the whole range, the periodic orbit is elliptic ($|\mu_i|=1$) and for $n_t \sim 0.5$ the exact results indicates that the orbit undergoes a period doubling bifurcation (marked by □).

form (dashed line) with the exact value (solid line) for one of the branches of periodic orbits (see Sec. IV D). Note that both curves predict that a pair of characteristic multipliers will meet and pass each other at -1 on the unit circle (period doubling bifurcation) for n_t around 0.4. In the whole range of the figure, the moduli of the characteristic multipliers is 1, so that the periodic orbit is elliptic.

D. Symmetric periodic solutions: Stability and bifurcations

As the system is invariant under rotations, we change our coordinate system to a rotating one and write

$$z(t)=(a(t),b(t),c(t),d(t))=e^{i\omega t}(A(t),B(t),C(t),D(t)), \tag{14}$$

with $\omega \neq 0$ being the angular velocity of the rotating frame to be determined. In these new coordinates the system is

$$\begin{aligned} \dot{A} &= i(B-\omega A), \\ \dot{B} &= i(A+C-\omega B), \\ \dot{C} &= i(B+D-\omega C)-i(C\overline{C})C, \\ \dot{D} &= i(C-\omega D). \end{aligned} \tag{15}$$

The equilibrium points of Eqs. (15) are now *symmetric periodic orbits* of the original system (5). These kind of solutions are also called *rotating waves* or *relative equilibria*. Recall from the Introduction that the factorization (14) is exactly the separation of variables that leads to the self-consistent Hartree solution. At this point, it is worthwhile to highlight that the standard self-consistent Hartree approximation chooses a very particular trajectory from those allowed by the vector field (5), one in which the time and the spatial dependence are factorized and it is invariant under the symmetry.

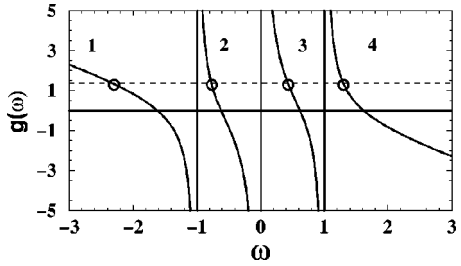

FIG. 4. Plot of the function $g(\omega)$ [Eq. (16)]. as a function of the frequency of the periodic orbit. For a given value of $|c|^2$, there are always exactly four different frequencies that belong to the four families of periodic orbits (hollow circles). Each of them will have different values of H and n_t. Close to the empty-state vector ($n_t \to 0$), the four branches tend to the values of the linear case $(-\phi,-1/\phi,1/\phi,\phi)$.

The stationary solutions of Eqs. (15) fulfill the following equations:

$$A_0=\frac{C_0}{\omega^2-1}, \quad B_0=\frac{\omega}{\omega^2-1}C_0, \quad D=\frac{C_0}{\omega},$$

$$|C_0|^2=-\frac{(\omega^2-\phi^2)\left(\omega^2-\dfrac{1}{\phi^2}\right)}{\omega(\omega^2-1)} := g(\omega). \tag{16}$$

For system (15), the Hamiltonian function is $\hat{H}=H-\omega n_t$; the remainder gives rise to extra contributions in the equations that are usually called Coriolis forces. If we express $\hat{H}$ in terms of ω, we get $g(\omega)/2$, which means that by choosing a rotating frame whose angular velocity matches the ω of the rotating wave, we eliminate the kinetic contribution and the energy is just the potential term.

A plot of $g(\omega)$ is shown in Fig. 4. The values of ω allowed by Eqs. (16) are those corresponding to the positive values of $g(\omega)$; the negative part would correspond to the attractive case ($U<0$) in Eqs. (4). For any value of $|c|^2$ we have always four solutions for Eqs. (16), corresponding to four different symmetric periodic solutions, and each of them will have a different value of n_t and H. The branches of $\omega>0$ and $\omega<0$ correspond to periodic solutions with different orientations. The function $g(\omega)$ has interesting symmetry properties, namely $g(1/\omega)=-g(\omega)$ and $g(-\omega)=-g(\omega)$, indicating that the attractive case can be mapped into the repulsive one.

The stability of system (15) has been analytically investigated by linearizing around the periodic solution (16). Taking $C_0=\sqrt{g(\omega)}e^{ik_0}$ and changing the origin of the coordinates to the equilibrium point, $\mathcal{A}=A-A_0$, $\mathcal{B}=B-B_0$, $\mathcal{C}=C-C_0$, and $\mathcal{D}=D-D_0$, we get the following system:

$$\dot{\mathcal{A}}=i(\mathcal{B}-\omega\mathcal{A}),$$

$$\dot{\mathcal{B}}=i(\mathcal{A}+\mathcal{C}-\omega\mathcal{B}),$$

$$\dot{\mathcal{C}}=i\{\mathcal{B}+\mathcal{D}-[\omega+2g(\omega)]\mathcal{C}-g(\omega)e^{2ik_0}\overline{\mathcal{C}}-\sqrt{g(\omega)}e^{-ik_0}\mathcal{C}^2 - 2\sqrt{g(\omega)}e^{ik_0}\mathcal{C}\overline{\mathcal{C}}-\overline{\mathcal{C}}^2\}, \tag{17}$$

$$\dot{\mathcal{D}}=i(\mathcal{C}-\omega\mathcal{D}).$$

The dependence on the phase k_0 can be eliminated by scaling each variable by e^{ik_0}. The linear part of Eqs. (17) can be written as

$$\dot{\mathcal{Z}}=iL\mathcal{Z}+iM\overline{\mathcal{Z}} \tag{18}$$

with L and M, 4×4 real matrices, and $\mathcal{Z}=(A,B,C,D)$,

$$L=\begin{pmatrix} -\omega & 1 & 0 & 0 \\ 1 & -\omega & 1 & 0 \\ 0 & 1 & -\omega-2g(\omega) & 1 \\ 0 & 0 & 1 & -\omega \end{pmatrix},$$

$$M=\begin{pmatrix} 0 & 0 & 0 & 0 \\ 0 & 0 & 0 & 0 \\ 0 & 0 & -g(\omega) & 0 \\ 0 & 0 & 0 & 0 \end{pmatrix}. \tag{19}$$

Separating in real and imaginary parts ($\mathcal{Z}=\mathcal{Z}_R+i\mathcal{Z}_I$,) the system is

$$\begin{pmatrix} \dot{\mathcal{Z}}_R \\ \dot{\mathcal{Z}}_I \end{pmatrix}=\begin{pmatrix} \mathcal{O} & M-L \\ M+L & \mathcal{O} \end{pmatrix}\begin{pmatrix} \mathcal{Z}_R \\ \mathcal{Z}_I \end{pmatrix}, \tag{20}$$

where $\mathcal{O}$ is a 4×4 zero matrix. If $\binom{u_1}{u_2}$ is an eigenvector of the 8×8 matrix with eigenvalue λ, then u_1 and u_2 satisfy the following four-dimensional equations:

$$(M-L)u_2=\lambda u_1, \tag{21}$$

$$(M+L)u_1=\lambda u_2, \tag{22}$$

which can be folded into a single eigenvalue equation,

$$(M+L)(M-L)u_2=\lambda^2 u_2. \tag{23}$$

Summarizing our analysis, the original system of eight ordinary differential equations (5) has been rewritten in a rotating frame with a constant angular velocity that depends on the energy of the system; the linearization of the resulting system can be folded to a four-dimensional system that reflects the Hamiltonian structure of the original system. The characteristic multipliers (μ) of the symmetric periodic orbit can be readily computed as the exponential of the characteristic exponent times the period of the orbit and for each eigenvalue of the folded system (λ^2). We get one pair of ($\pm\lambda$) and the corresponding multipliers,

$$\mu_i=e^{\pm T\lambda_i}=e^{\pm 2\pi\lambda_i/\omega}. \tag{24}$$

The rank of $M-L$ is 3 and the rank of $M+L$ is 4, i.e., there is just one eigenvalue equal to zero, which leads to two exponents equal to zero and two characteristic multipliers equal to 1 for every ω. These two $+1$ reflect, as expected, the Hamiltonian character and the fact that we are studying a periodic orbit; the characteristic multiplier along the direction of the orbit has to be 1 and the periodic orbits belong to a continuous family. Note that for the case of two *independent* constants of motion, a classical theorem by Poincaré [18] ensures *four* characteristic multipliers equal to 1 and in our case we just find *two*. The explanation for our results is that along the *rotating solutions* the gradient of the Hamiltonian and the gradient of the total charge are linearly dependent and the above-mentioned theorem does not apply. The remaining three eigenvalues of the folded system can either all be real or one pair of complex conjugate and one real.

If the eigenvalues of Eq. (23) are real and positive, then the periodic orbit is hyperbolic ($\lambda=\pm\sigma$ with $\sigma\in\mathcal{R}$) and the multipliers are inside and outside the unit circle, respectively. If they are real and negative, then the periodic orbit is elliptic ($\lambda=\pm i\mu$ with $\mu\in\mathcal{R}$), the multipliers have moduli equal to 1, and it is surrounded by quasiperiodic tori. If they are with a nonzero imaginary part, then the characteristic exponents must appear in two conjugate pairs ($\lambda=\pm\sigma\pm i\mu$ with $\mu,\sigma\in\mathcal{R}$). The stable and unstable manifold are both two dimensional, spiral around the periodic orbit, and under certain conditions we might find entanglement. A special case occurs for $T\mu=k\pi$ with $k\in\mathcal{N}$. Then the two pairs of multipliers cross the real axis and the orbit is hyperbolic.

In the linear case [$U=0\Rightarrow g(\omega)=0$] the matrix to be diagonalized in Eq. (23) is $-L^2$. L is real and symmetric and its eigenvalues are real; therefore, the eigenvalues of $-L^2$ are negative. As the eigenvalues are continuous functions of ω, the symmetric periodic orbits are always *elliptic* close to the origin and this stability analysis agrees with the normal form result of Sec. IV C.

According to our analysis, the symmetric periodic orbit undergoes three kinds of local bifurcations, as follows.

(i) One pair of multipliers coincides with a q root of unity ($q\in\mathcal{N}$). Depending on the argument of the characteristic multipliers we have a double $+1$ ($q=1$), period doubling ($q=2$), or q-subharmonic bifurcation ($q>2$).

(ii) Two pairs of multipliers meet on the unit circles and pass each other.

(iii) Two pairs of multipliers meet and split departing the unit circle with the same argument (loxodromic bifurcation).

We present our results in two figures. In Fig. 5, we plot the argument of the characteristic multipliers for the four branches of $g(\omega)$ (or four families of symmetric periodic orbits) computed by diagonalizing the 4×4 matrix. The vertical axis run from $-\pi$ to $+\pi$ and the horizontal axis are the total charge in the system (n_t), which we use as a continuation parameter. The double $+1$ that is always present has been deleted for the sake of clarity in all the figures, i.e., we display just the significant multipliers.

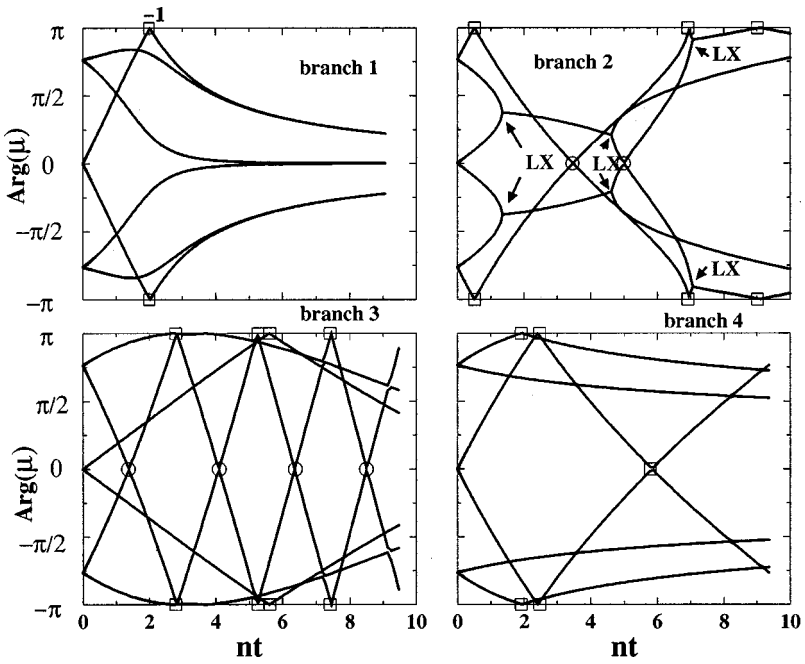

FIG. 5. Argument of the characteristic multipliers for the four branches as a function of the total charge (n_t). The double $+1$ are marked by circles, the period doubling by squares, and the loxodromic bifurcation is labeled as LX in branch 2.

In branches 1, 3, and 4, the symmetric periodic orbits are always elliptic but undergo q-subharmonic bifurcations as n_t is varied. The most interesting branch seems to be the second one, which is plotted in Fig. 6 along with the moduli of the multipliers in the upper panel. The orbit undergoes, in the range of the figure, two double $+1$ bifurcations (marked by squares), four loxodromic bifurcations (marked by LX), and three period-doubling bifurcations (squares). Note that in Fig. 6 the symmetric periodic orbit that has left the unit circle at $n_t \sim 7$ via a loxodromic bifurcation undergoes a subsequent period doubling bifurcation and the symmetric periodic orbit is hyperbolic for $n_t \sim 9$. The lower panel of that figure correspond to a test function of a numerical continuation analysis using AUTO [19] that detects just the double $+1$ bifurcation. At this bifurcation point, a branch of tori of nonsymmetric orbits is born whose continuation is difficult and will be discussed elsewhere [20].

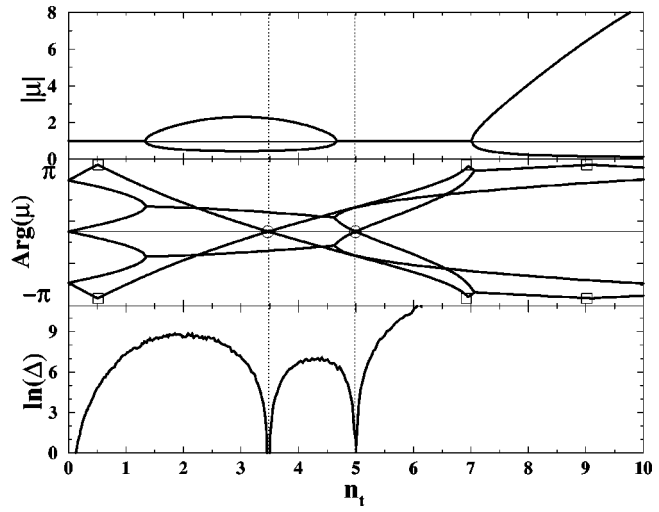

FIG. 6. Moduli (top) and arguments (middle) for the eight characteristic multipliers for branch 2. Bottom panel is the bifurcation function in the numerical continuation as a function of n_t. We have marked the double $+1$ bifurcation by hollow circles and the period doubling by squares.

V. CONCLUSIONS

In this work, we have investigated a dynamical point of view of the mean field approximation in the specific example of a tight-binding four-site system with a nonlinear interaction in one of the sites. We have made use of the fact that the discrete mean field Schrödinger equation can be formulated as a classical Hamiltonian and the conservation of charge in a closed system is associated with a rotation symmetry. The numerical and bifurcation analysis shows that the origin of the chaotic behavior in the continuum and discrete model is related to the nonintegrability of the Hamiltonian problem. We have detected three kinds of local bifurcations of periodic orbits and identified the q-subharmonic and the loxodromic bifurcation as the organizing centers of the dynamics.

The exact many-body problem is described by a linear Schrödinger equation and cannot be chaotic for any finite-number of degrees of freedom. Chaotic behavior may appear in the thermodynamic limit [21,22]. Our analysis shows that the structure of the variational mean field approach is failing to properly describe the correlation of the charged particles in the many-body problem, and that the dynamical behavior has to be taken into account to improve the approximation.

ACKNOWLEDGMENTS

The authors wish to acknowledge L. L. Bonilla, F. J. Muñoz Almaraz, E. Doedel, and A. Vanderbauwhede for helpful discussions. This work was partially supported by the Junta de Andalucía, DGICyT, and NATO Grant No. CRG-972260.

[1] N. W. Ashcroft and N. D. Mermin, *Solid State Physics* (Saunders College, Philadelphia, 1976).
[2] G. Jona-Lasinio, C. Presilla, and F. Capasso, Phys. Rev. Lett. **68**, 2269 (1992).
[3] C. Presilla, G. Jona-Lasinio, and F. Capasso, in *Chaos in Mesoscopic Physics*, edited by G. Casati and H. A. Cerdeira (World Scientific, Singapore, 1993).
[4] J. Hubbard, Proc. R. Soc. London, Ser. A **276**, 238 (1963); *The Hubbard Model, Its Physics and Mathematical Physics*, edited by D. Bareswyl, D. K. Campbell, J. M. P. Carmelo, F. Guinea, and E. Louis, Nato Advanced Study Insitute Series B: Physics, Vol. 343 (Plenum, New York, 1995).
[5] The Lyapunov exponents have been computed with the code *easynum* written by Pavel Pokorny (http://staff.vscht.cz/mat/Pavel.Pokorny).
[6] K. R. Meyer and G. R. Hall, *Introduction to Hamiltonian Dynamical Systems and the N-body Problem*, Applied Mathematical Sciences, Vol. 90 (Springer-Verlag, New York, 1991).
[7] R. Abraham and J. Marsden, *Foundations of Mechanics*, 2nd ed. (Addison-Wesley, New York, 1978).
[8] J. Galán and J. A. Vergés, Phys. Rev. B **44**, 10093 (1991).
[9] J. Galán, J. A. Vergés, and A. Martíin Rodero, Phys. Rev. B **48**, 13654 (1998).
[10] J. A. Sanders and F. Verhulst, *Averaging Methods in Nonlinear Dynamical Systems*, Applied Mathematical Sciences Vol. 59 (Springer-Verlag, New York, 1985).
[11] C. Simó, in *Cent ans après les Méthodes Nouvelles H. Poincaré* (Société Mathématique de France, Paris, 1996),pp. 1–23.
[12] C. Simó, G. Gómez, À. Jorba, and J. Masdemont, in *From Newton to Chaos*, edited by A. E. Roy and B. A. Stevens (Plenum, New York, 1995), pp. 343–370.
[13] A. Giorgilli, A. Delshams, E. Fontich, L. Galgani, and C. Simó, J. Diff. Eqns. **77**, 167 (1989).
[14] À. Jorba and C. Simó, in *Hamiltonian Mechanics, Integrability and Chaotic Behavior*, edited by J. Seimenis, NATO Advanced Study Institute Series B: Physics, Vol. 331 (Plenum, New York, 1994), pp. 245–252.
[15] À. Jorba and J. Villanueva, Physica D **114**, 197 (1998).
[16] S. Chow, C. Li, and D. Wang, *Normal Form and Bifurcation of Planar Vector Fields* (Cambridge University Press, New York, 1994).
[17] J. Montaldi, M. Roberts, and I. Stewart, Philos. Trans. R. Soc. London, Ser. A **325**, 237 (1988); Nonlinearity **3**, 695 (1990); **3**, 731 (1990).
[18] H. Poincaré, *Les Methodes Nouvelles de la Mechanique Celeste* (Gauthier-Villar, Paris, 1899).
[19] E. J. Doedel and X. J. Wang, AUTO94: Software for continuation and bifurcation problems in ordinary differential equations (1995).
[20] F. J. Muñoz Almaraz, E. Freire, E. J. Doedel, A. Vanderbauwhede, and J. Galán (unpublished).
[21] G. Jona-Lasinio and C. Presilla, Phys. Rev. Lett. **77**, 4322 (1996).
[22] P. Castiglione, G. Jona-Lasinio, and C. Presilla, J. Phys. A **29**, 6169 (1996).